Using stromal cells established from a tumor-like lesion of a NOMID patient, Almeida *et al.* demonstrated that activation of the cAMP/PKA/CREB pathway leads to caspase-1 activation, release of IL-1β, and consequently the proliferation of bone stromal cells. This suggests that bone lesions in NOMID are caused in an NLRP3 inflammasome-dependent manner. One explanation for the discrepancy between their data and ours is that no disease-causing *NLPR3* mutation was identified in the patient studied in this previous report; therefore, an unknown genetic alteration may have caused the NOMID phenotype. Another explanation is that different cell types were analyzed in the two studies. The previous study analyzed bone stromal cells established from a tumor-like lesion that might have been a heterogeneous population, while we focused on a single cell type, namely, chondrocytes. The lack of environmental factors and interactions with other cell populations in our model might have eliminated some contributions of the NLRP3 inflammasome and IL-1β pathway that occur in NOMID patients. Furthermore, our observations relied on an artificial differentiation system in which iPS cells were first differentiated into cells of neural crest character and then into chondrocytes by culture in the presence of various exogenous factors. Abnormal epiphyseal growth is specifically observed around the knee joints of NOMID patients; therefore, additional events might be required to trigger abnormal chondrocyte proliferation *in vivo*. It is also possible that specific factors produced by surrounding cells in non-affected joints prevent mutant chondrocytes manifesting their phenotype. Further analyses of patients or patient-derived samples would provide a better understanding of the pathophysiology of arthropathy in

NOMID.

The interaction between cAMP and NLRP3 has been studied in monocytes/macrophages, in which the NLRP3 inflammasome is activated following binding of extracellular Ca^{2+} to Ca^{2+}-sensing receptors (CaSRs) (37, 38). One study reported that an increase in extracellular Ca^{2+} is detected by CaSRs, which leads to phospholipase C activation and subsequently the release of Ca^{2+} from the endoplasmic reticulum and downregulation of cAMP. cAMP binds directly to NLRP3 and inhibits assembly of the NLRP3 inflammasome. Therefore, this decrease in the level of intracellular cAMP relieves this inhibition and thereby induces activation of the NLRP3 inflammasome (37). On the other hand, another study reported that an increase in the extracellular Ca^{2+} concentration induces an increase in the intracellular Ca^{2+} concentration, thereby leading to activation of the NLRP3 inflammasome, and this mechanism requires the CaSRs GPRC6A and CaSR, but not the downregulation of cAMP (38). Thus, the effects of cAMP on the NLRP3 inflammasome in monocytes/macrophages remain controversial. In the chondrocyte differentiation system used in the current study, mutated NLRP3 caused *SOX9* overexpression via the cAMP/PKA/CREB pathway, which is at odds with the relationship between cAMP and activation of the NLRP3 inflammasome in monocytes/macrophages. This discrepancy might be explained by the absence of other NLRP3 inflammasome components, such as ASC and procaspase-1, in the chondrocytes generated in the current study. Further analysis is needed to determine why cAMP/PKA/CREB signaling elicits different effects on mutated NLRP3 in chondrocytes and monocytes/macrophages, as well as how

intracellular cAMP is upregulated in chondrocytes derived from mutant iPS cells.

There have been many reports on the differentiation of chondrocytes from embryonic stem (ES)/iPS cells (39-41). However, previously, it was difficult to differentiate a sufficient number of chondrocytes with a relatively mature phenotype from ES/iPS cells, especially human ES/iPS cells. We have recently established a cartilage differentiation system in which iPS cells first differentiate into cells of neural crest character and then into chondrocytes, which enabled us to obtain a large number of chondrocytes with the phenotype of growth plate cartilage chondrocytes. An important aspect of the current study is that this differentiation system can generate a large number of chondrocytes that could share functional property causing the arthropathy observed in NOMID. This system could thereby be used to screen for novel therapeutic agents.

In conclusion, we showed that *SOX9* is overexpressed via the cAMP/PKA/CREB signaling pathway in chondrocytes with disease-causing mutations in *NLRP3*, and this causes overproduction of ECM independently of the NLRP3 inflammasome. iPS cell technology was used to elucidate the role of chondrocytes in the pathophysiology of the human disease NOMID.

Acknowledgments

We are grateful to K. Hayakawa, M. Fukuta, S. Nagata, and M. Hiraga of Kyoto University for technical assistance and to N. Kambe of Chiba University for critically reading this manuscript.

Authors' Contributions

K.Y., M.I., K.U., R.N., and J.T. designed the experiments and prepared the manuscript. K.Y., S.N., K.I., K.H., and T.K. performed the experiments. H.O., T.T., Y.M., A.N., M.K.S., T.Y., O.O., N.N., and T.N. gave technical support and conceptual advice. T.H. and J.T. supervised the project.

Competing Financial Interests

The authors have declared that no conflict of interest exists.

References

1. Kufer TA, Sansonetti PJ. NLR functions beyond pathogen recognition. Nature immunology. 2011;12(2):121-8.

2. Hoffman HM, Mueller JL, Broide DH, Wanderer AA, Kolodner RD. Mutation of a new gene encoding a putative pyrin-like protein causes familial cold autoinflammatory syndrome and Muckle-Wells syndrome. Nature genetics. 2001;29(3):301-5.

3. Tanaka N, Izawa K, Saito MK, Sakuma M, Oshima K, Ohara O, et al. High incidence of NLRP3 somatic mosaicism in patients with chronic infantile neurologic, cutaneous, articular syndrome: results of an International Multicenter Collaborative Study. Arthritis and rheumatism. 2011;63(11):3625-32.

4. Feldmann J, Prieur AM, Quartier P, Berquin P, Certain S, Cortis E, et al. Chronic infantile neurological cutaneous and articular syndrome is caused by mutations in CIAS1, a gene highly expressed in polymorphonuclear cells and chondrocytes. American journal of human genetics. 2002;71(1):198-203.

5. Latz E, Xiao TS, Stutz A. Activation and regulation of the inflammasomes. Nature reviews Immunology. 2013;13(6):397-411.

6. Gattorno M, Martini A. Beyond the NLRP3 inflammasome: autoinflammatory diseases reach adolescence. Arthritis and rheumatism. 2013;65(5):1137-47.

7. Bauernfeind FG, Horvath G, Stutz A, Alnemri ES, MacDonald K, Speert D, et al. Cutting edge: NF-kappaB activating pattern recognition and cytokine receptors license NLRP3 inflammasome activation by regulating NLRP3 expression. Journal of immunology. 2009;183(2):787-91.

8. Mariathasan S, Weiss DS, Newton K, McBride J, O'Rourke K, Roose-Girma M, et al. Cryopyrin activates the inflammasome in response to toxins and ATP. Nature. 2006;440(7081):228-32.

9. Hoffman HM, Rosengren S, Boyle DL, Cho JY, Nayar J, Mueller JL, et al. Prevention of cold-associated acute inflammation in familial cold autoinflammatory syndrome by interleukin-1 receptor antagonist. The Lancet. 2004;364(9447):1779-85.

10. Hawkins PN, Lachmann HJ, McDermott MF. Interleukin-1-receptor antagonist in the Muckle-Wells syndrome. The New England journal of medicine. 2003;348(25):2583-4.

11. Lachmann HJ, Kone-Paut I, Kuemmerle-Deschner JB, Leslie KS, Hachulla E, Quartier P, et al. Use of canakinumab in the cryopyrin-associated periodic syndrome. The New England journal of medicine. 2009;360(23):2416-25.

12. Arostegui JI, Lopez Saldana MD, Pascal M, Clemente D, Aymerich M, Balaguer F, et al. A somatic NLRP3 mutation as a cause of a sporadic case of chronic infantile neurologic, cutaneous, articular syndrome/neonatal-onset multisystem inflammatory disease: Novel evidence of the role of low-level mosaicism as the pathophysiologic mechanism underlying mendelian inherited diseases.

Arthritis and rheumatism. 2010;62(4):1158-66.

13. Hill SC, Namde M, Dwyer A, Poznanski A, Canna S, Goldbach-Mansky R. Arthropathy of neonatal onset multisystem inflammatory disease (NOMID/CINCA). Pediatric radiology. 2007;37(2):145-52.

14. Mackie EJ, Tatarczuch L, Mirams M. The skeleton: a multi-functional complex organ: the growth plate chondrocyte and endochondral ossification. The Journal of endocrinology. 2011;211(2):109-21.

15. Goldring MB, Tsuchimochi K, Ijiri K. The control of chondrogenesis. Journal of cellular biochemistry. 2006;97(1):33-44.

16. Bonar SL, Brydges SD, Mueller JL, McGeough MD, Pena C, Chen D, et al. Constitutively activated NLRP3 inflammasome causes inflammation and abnormal skeletal development in mice. PloS one. 2012;7(4):e35979.

17. Tanaka T, Takahashi K, Yamane M, Tomida S, Nakamura S, Oshima K, et al. Induced pluripotent stem cells from CINCA syndrome patients as a model for dissecting somatic mosaicism and drug discovery. Blood. 2012;120(6):1299-308.

18. Umeda K, Zhao J, Simmons P, Stanley E, Elefanty A, Nakayama N. Human chondrogenic paraxial mesoderm, directed specification and prospective isolation from pluripotent stem cells. Scientific reports. 2012;2:455.

19. Nasu A, Ikeya M, Yamamoto T, Watanabe A, Jin Y, Matsumoto Y, et al. Genetically matched human iPS cells reveal that propensity for cartilage and bone differentiation differs with clones, not cell type of origin. PloS one. 2013;8(1):e53771.

20. Sakai H, Okafuji I, Nishikomori R, Abe J, Izawa K, Kambe N, et al. The CD40-CD40L axis and IFN-gamma play critical roles in Langhans giant cell formation. International immunology. 2012;24(1):5-15.

21. Aoyama T, Okamoto T, Nagayama S, Nishijo K, Ishibe T, Yasura K, et al. Methylation in the core-promoter region of the chondromodulin-I gene determines the cell-specific expression by regulating the binding of transcriptional activator Sp3. The Journal of biological chemistry. 2004;279(27):28789-97.

22. Ushita M, Saito T, Ikeda T, Yano F, Higashikawa A, Ogata N, et al. Transcriptional induction of SOX9 by NF-kappaB family member RelA in chondrogenic cells. Osteoarthritis and cartilage / OARS, Osteoarthritis Research Society. 2009;17(8):1065-75.

23. Kajita Y, Kato T, Jr., Tamaki S, Furu M, Takahashi R, Nagayama S, et al. The transcription factor Sp3 regulates the expression of a metastasis-related marker of sarcoma, actin filament-associated protein 1-like 1 (AFAP1L1). PloS one. 2013;8(1):e49709.

24. Sandelin A, Alkema W, Engstrom P, Wasserman WW, Lenhard B. JASPAR: an open-access database for eukaryotic transcription factor binding profiles. Nucleic acids research. 2004;32(Database

issue):D91-4.

25. Saito M, Fujisawa A, Nishikomori R, Kambe N, Nakata-Hizume M, Yoshimoto M, et al. Somatic mosaicism of CIAS1 in a patient with chronic infantile neurologic, cutaneous, articular syndrome. Arthritis and rheumatism. 2005;52(11):3579-85.

26. Saito M, Nishikomori R, Kambe N, Fujisawa A, Tanizaki H, Takeichi K, et al. Disease-associated CIAS1 mutations induce monocyte death, revealing low-level mosaicism in mutation-negative cryopyrin-associated periodic syndrome patients. Blood. 2008;111(4):2132-41.

27. Aksentijevich I, Nowak M, Mallah M, Chae JJ, Watford WT, Hofmann SR, et al. De novo CIAS1 mutations, cytokine activation, and evidence for genetic heterogeneity in patients with neonatal-onset multisystem inflammatory disease (NOMID): a new member of the expanding family of pyrin-associated autoinflammatory diseases. Arthritis and rheumatism. 2002;46(12):3340-8.

28. Akiyama H, Lefebvre V. Unraveling the transcriptional regulatory machinery in chondrogenesis. Journal of bone and mineral metabolism. 2011;29(4):390-5.

29. Kim Y, Murao H, Yamamoto K, Deng JM, Behringer RR, Nakamura T, et al. Generation of transgenic mice for conditional overexpression of Sox9. Journal of bone and mineral metabolism. 2011;29(1):123-9.

30. Cucchiarini M, Orth P, Madry H. Direct rAAV SOX9 administration for durable articular cartilage repair with delayed terminal differentiation and hypertrophy in vivo. Journal of molecular medicine. 2013;91(5):625-36.

31. Cucchiarini M, Thurn T, Weimer A, Kohn D, Terwilliger EF, Madry H. Restoration of the extracellular matrix in human osteoarthritic articular cartilage by overexpression of the transcription factor SOX9. Arthritis and rheumatism. 2007;56(1):158-67.

32. Tew SR, Li Y, Pothacharoen P, Tweats LM, Hawkins RE, Hardingham TE. Retroviral transduction with SOX9 enhances re-expression of the chondrocyte phenotype in passaged osteoarthritic human articular chondrocytes. Osteoarthritis and cartilage / OARS, Osteoarthritis Research Society. 2005;13(1):80-9.

33. Carroll SH, Ravid K. Differentiation of mesenchymal stem cells to osteoblasts and chondrocytes: a focus on adenosine receptors. Expert reviews in molecular medicine. 2013;15:e1.

34. Huang W, Zhou X, Lefebvre V, de Crombrugghe B. Phosphorylation of SOX9 by cyclic AMP-dependent protein kinase A enhances SOX9's ability to transactivate a Col2a1 chondrocyte-specific enhancer. Molecular and cellular biology. 2000;20(11):4149-58.

35. Tsuda M, Takahashi S, Takahashi Y, Asahara H. Transcriptional co-activators CREB-binding protein and p300 regulate chondrocyte-specific gene expression via association with Sox9. The Journal of biological chemistry. 2003;278(29):27224-9.

36. Yoon YM, Oh CD, Kang SS, Chun JS. Protein kinase A regulates chondrogenesis of

mesenchymal cells at the post-precartilage condensation stage via protein kinase C-alpha signaling. Journal of bone and mineral research : the official journal of the American Society for Bone and Mineral Research. 2000;15(11):2197-205.

37. Lee GS, Subramanian N, Kim AI, Aksentijevich I, Goldbach-Mansky R, Sacks DB, et al. The calcium-sensing receptor regulates the NLRP3 inflammasome through Ca2+ and cAMP. Nature. 2012;492(7427):123-7.

38. Rossol M, Pierer M, Raulien N, Quandt D, Meusch U, Rothe K, et al. Extracellular Ca2+ is a danger signal activating the NLRP3 inflammasome through G protein-coupled calcium sensing receptors. Nature communications. 2012;3:1329.

39. Barberi T, Willis LM, Socci ND, Studer L. Derivation of multipotent mesenchymal precursors from human embryonic stem cells. PLoS medicine. 2005;2(6):e161.

40. Kawaguchi J, Mee PJ, Smith AG. Osteogenic and chondrogenic differentiation of embryonic stem cells in response to specific growth factors. Bone. 2005;36(5):758-69.

41. zur Nieden NI, Kempka G, Rancourt DE, Ahr HJ. Induction of chondro-, osteo- and adipogenesis in embryonic stem cells by bone morphogenetic protein-2: effect of cofactors on differentiating lineages. BMC developmental biology. 2005;5:1.

Figure Legends

Figure 1. Chondrocytes are successfully differentiated from iPS cells *in vitro*. **A,** Schematic presentation of the culture conditions used to differentiate chondrocytes from iPS cells. **B,** Immunohistochemical staining of chondrocytes differentiated from iPS cells. From left to right, Alcian blue staining of 2D micromass, Alcian blue staining of 3D pellet, higher magnification images of Alcian blue staining of 3D pellet, and anti-COL2 antibody staining of 3D pellet and mouse bladder (negative control). White scale bars: 2.0 mm; black scale bars: 0.2 mm. **C,** Quantitative analysis of the sizes of chondrocyte tissue masses in 2D micromass cultures (left panel) and 3D pellet cultures. **D**, Cartilage-specific gene expression in 3D pellet cultures. mRNA expression of each gene is shown relative to that in human cartilage (*SOX9*, *COL2A1*, *ACAN*, and *COMP*) or the osteosarcoma cell line ANOS (*IHH*, *MMP13*, *COL10A1*, and *VEGFA*), which were both set at 1. Bars and error bars represent the mean and SEM, respectively, of three independent clones, from which duplicate measurements (**C**) or triplicated measurements (**D**) were obtained. Data are representative of three independent experiments. * indicates $p<0.05$. Data shown used iPS cells from patient 1 (p.Tyr570Cys); similar data were obtained using iPS cells from patient 2 (p.Gly307Ser).

Figure 2. The formation of large cartilaginous masses by mutant iPS cells is owing to the overproduction of ECM, not to increased cell proliferation. **A,** Growth curves of chondroprogenitor cells differentiated from mutant and WT iPS cells. Error bars represent the SEM of three independent clones, from which

duplicate measurements were obtained. **B and C,** DNA concentration, GAG concentration, and the ratio of GAG concentration to DNA concentration in 2D micromass (**B**) and 3D pellet (**C**) cultures. Bars and error bars show the mean and SEM, respectively, of three independent clones. Triplicate (**B**) or duplicate (**C**) measurements were obtained. Data are representative of three independent experiments with consistent results. * indicates $p<0.05$.

Figure 3. *In vivo* maturation of 3D cell pellets. **A,** Images of 3D cell pellets derived from mutant (upper panel) or WT (lower panel) iPS cells following transplantation into immunodeficient mice. Images from left to right show gross appearance, HE staining, Alcian blue staining, von Kossa staining, and higher magnification images of von Kossa staining. Red circles indicate bone/cartilage pellets in gel form. White scale bars: 2.0 mm; black scale bars: 0.2 mm. Data shown used iPS cells from patient 1; similar results were obtained using iPS cells from patient 2. **B,** Quantitative analysis of the size of pellets when they were transplanted (Day 38) and harvested (Day 66). Bars and error bars represent the mean and SEM, respectively, of three independent clones, from which duplicate measurements were obtained. Data are representative of three independent experiments. * indicates $p<0.05$.

Figure 4. The enhanced chondrogenesis of mutant iPS cells is independent of the NLRP3 inflammasome. The caspase-1 inhibitor Ac-YVAD-CHO (YVAD, 10 μM) or human recombinant IL-1Ra (1 μg/ml) were added to the 2D micromass cultures. As controls, cultures were incubated with DMSO or PBS containing

BSA. The diameter of the micromass (**B**), *SOX9* expression (**C**), DNA concentration, GAG concentration, and the ratio of GAG concentration to DNA concentration (**D**) were measured. Representative 2D micromass cultures are shown (**A**). Bars and error bars show the mean and SEM, respectively, of three independent clones. Triplicate measurements were obtained. Data are representative of three independent experiments. * indicates $p<0.05$. Data shown used iPS cells from patient 1; similar results were obtained using iPS cells from patient 2.

Figure 5. Expression of *SOX9* and *COL2A1* is upregulated in chondrocytes with mutated *NLRP3* during the chondroprogenitor cell stage. Expression of *SOX9*, *COL2A1*, *ACAN*, *COMP*, and *NLRP3* in each clone was measured in triplicate from Day −9 to 15. Expression levels of *SOX9*, *COL2A1*, *ACAN*, and *COMP* are shown relative to those in ANOS cells (set at 1), and the expression level of *NLRP3* is shown relative to that in peripheral blood mononuclear cells (PBMCs; set at 1). Bars and error bars show the mean and SEM, respectively, of three independent clones. Data are representative of three independent experiments with consistent results. * indicates $p<0.05$. Data shown used iPS cells from patient 1; similar results were obtained using iPS cells from patient 2.

Figure 6. *SOX9* upregulation in mutant NLRP3 chondrocytes is dependent on the cAMP/PKA/CREB pathway. **A,** *SOX9* promoter activity in mutant and WT chondroprogenitor cells following introduction of

mutations into its transcription factor-binding sites. **B,** *SOX9* promoter activity and expression in mutant and WT chondroprogenitor cells treated with forskolin or SQ22536. **C,** Effects of forskolin and SQ22536 on 3D pellets of mutant and WT cells. White scale bars: 2.0 mm. Both reagents were used at a concentration of 10 μM. **D,** The cAMP/PKA/CREB pathway is more active in mutant chondroprogenitor cells than in WT chondroprogenitor cells. cAMP concentration in mutant and WT iPS cells (Day 0) and chondroprogenitor cells (Day 15 and 36), and Western blot analysis of phosphorylated CREB (P-CREB) in mutant (MT1–3) and WT (WT1–3) chondroprogenitor cells. **E,** A schematic diagram summarizing the molecular mechanism elucidated in this study. Bars and error bars show the mean and SEM, respectively, of three independent clones. Triplicate (**A, B, D**) or duplicate (**C**) measurements were obtained. Data are representative of two independent experiments with consistent results. * indicates $p<0.05$. Data shown used iPS cells from patient 1; similar results were obtained using iPS cells from patient 2.

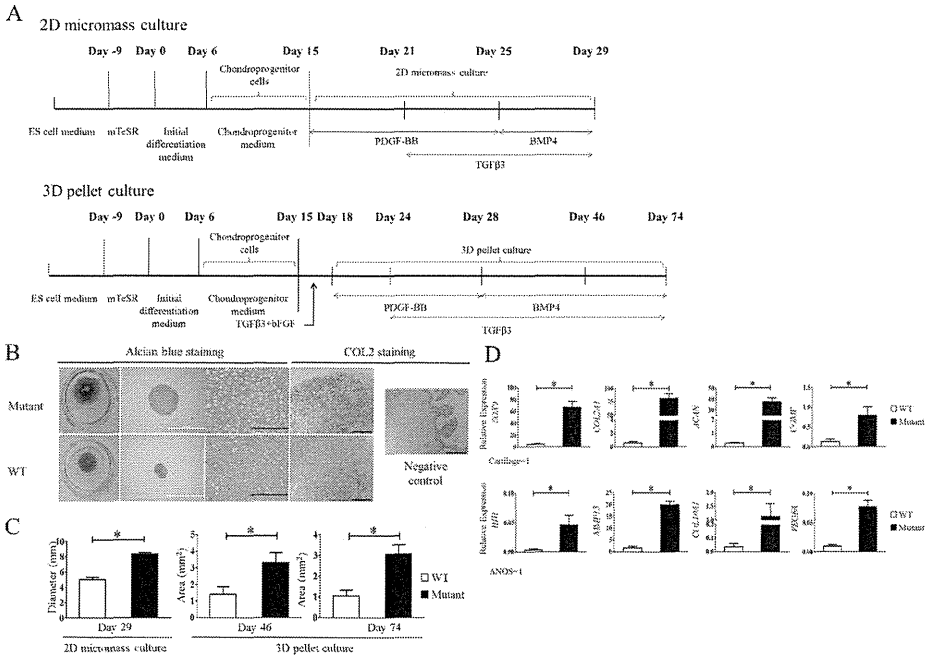

figure
201x142mm (300 x 300 DPI)

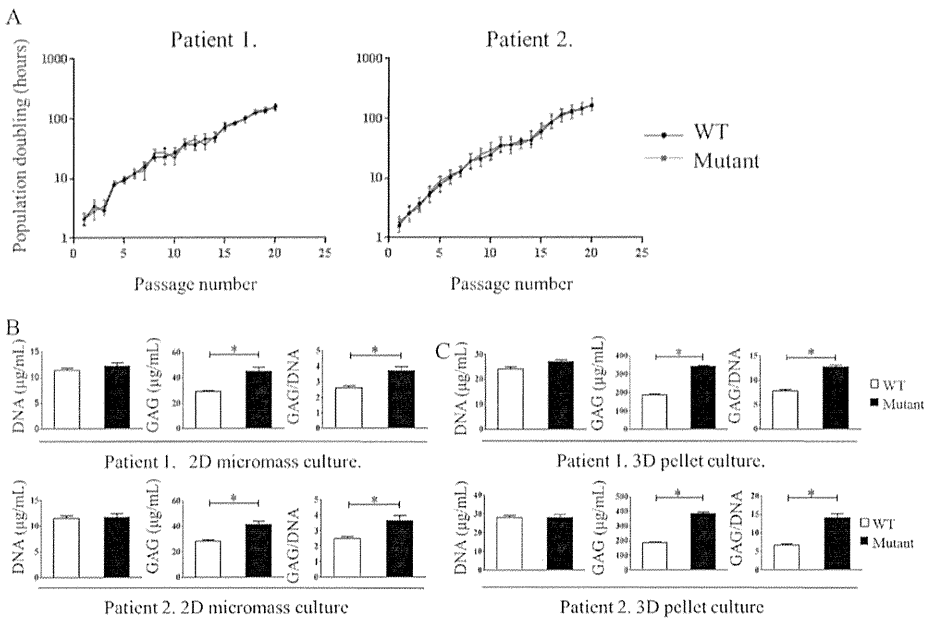

figure2
201x142mm (300 x 300 DPI)

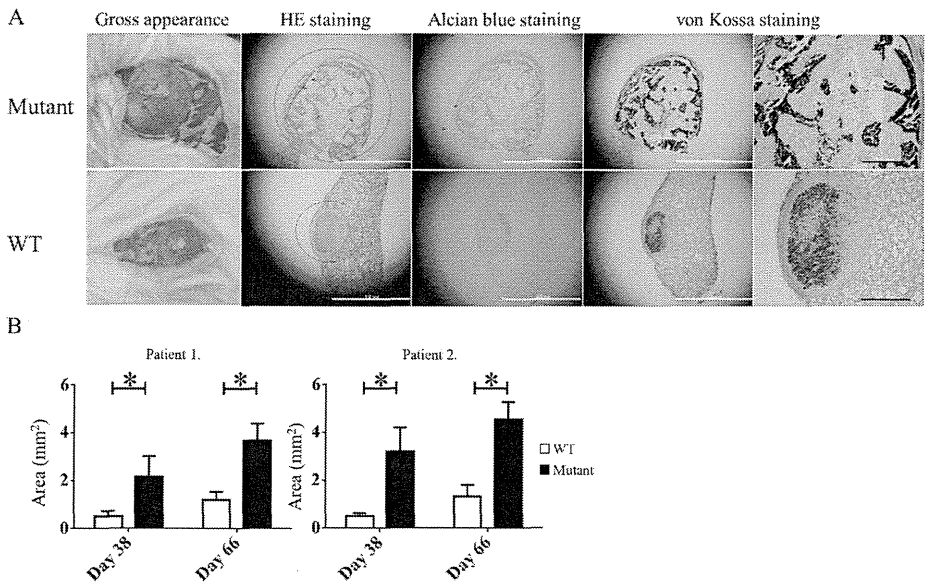

figure3
201x142mm (300 x 300 DPI)

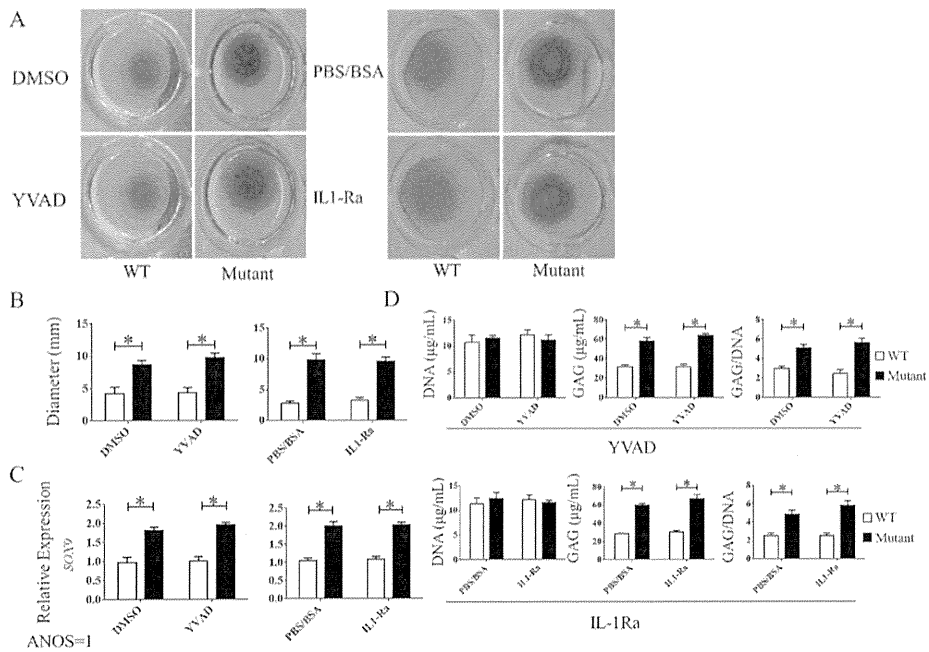

figure4
201x142mm (300 x 300 DPI)

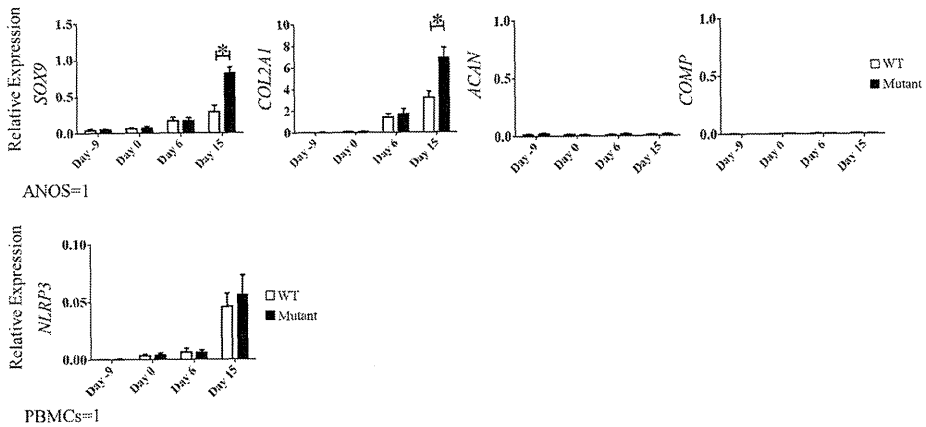

figure5
201x142mm (300 x 300 DPI)

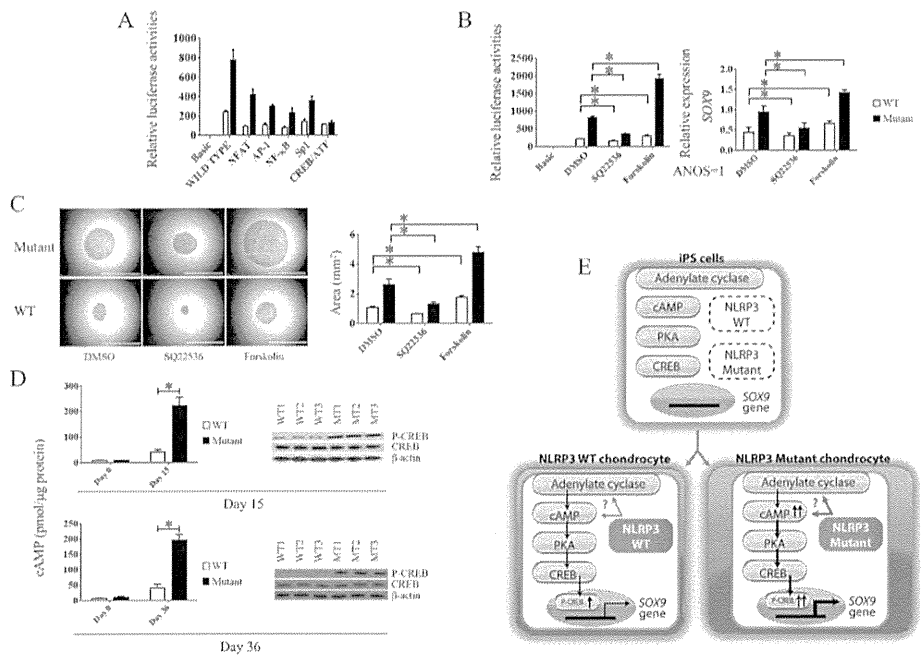

figure6
201x142mm (300 x 300 DPI)

Aldehyde dehydrogenase-2 polymorphism contributes to the progression of bone marrow failure in children with idiopathic aplastic anaemia

Aplastic anaemia is a syndrome of bone marrow failure (BMF) that is characterized by peripheral pancytopenia and marrow hypoplasia. Injury to haematopoietic stem cells (HSCs), such as immune-mediated cytotoxicity, can cause aplastic anaemia; the successful treatment of aplastic anaemia using immunosuppressive therapy (IST) supports this hypothesis (Kulagin *et al*, 2014). Another proposed mechanism is an intrinsic defect of HSCs, which is the presumed major cause of congenital BMF. However, this has not been definitively established in idiopathic aplastic anaemia.

The aldehyde dehydrogenases (ALDHs) are a group of enzymes that are involved in critically important biological processes, such as detoxification of exogenous and endogenous aldehydes. ALDH2 deficiency, resulting from a Glu504Lys substitution (rs671, c.1510G>A) in the *ALDH2* gene, is prevalent in the Japanese population. AA homozygotes show very low catalysis of aldehydes, and GA heterozygotes display strongly reduced catalysis compared with GG homozygotes. Recently, ALDH2 deficiency was shown to be associated with accelerated progression of BMF in Japanese patients with Fanconi anaemia (FA), the most frequent inherited cause of BMF (Hira *et al*, 2013).

We hypothesized that ALDH2 deficiency underlies the progression of BMF in patients with idiopathic aplastic anaemia as well as in FA patients.

Seventy-nine Japanese children aged ≤15 years, referred to our institution between January 1990 and April 2011, were included in this study. Patients were excluded if they had paroxysmal nocturnal haemoglobinuria (PNH), exposure to toxic chemicals, chromosomal fragility, or mutations in *TERC*, *TERT*, *SBDS* or *SH2D1A* (Liang *et al*, 2006; Wang *et al*, 2007). Disease severity was classified based on the criteria of the International Aplastic Anaemia Study Group (Camitta *et al*, 1975; Bacigalupo *et al*, 1988). The *ALDH2* Glu504Lys polymorphism was genotyped using a duplex polymerase chain reaction with confronting two-pair primers (Tamakoshi *et al*, 2003). Statistical analysis was performed using the Fisher's exact test and the Kruskal-Wallis test. Failure-free survival (defined by survival in the absence of relapse, additional therapy, PNH, or secondary malignancy) was analysed with the Kaplan-Meier method. All statistical analyses were conducted using JMP Pro 10·0·2 software (SAS Institute Inc., Cary, NC, USA). The study was approved by the ethics committee of Nagoya University Graduate School of Medicine.

The study included children whose disease type was classified as very severe (n = 10), severe (n = 40) and not severe (n = 29). Regarding the *ALDH2* Glu504Lys polymorphism, 40 children were genotyped as GG, 29 as GA, and 10 as AA (Table I). This distribution of the *ALDH2* polymorphism was not significantly different from the reported allele frequencies in the healthy Japanese population (Matsuo *et al*, 2006) (GG = 1141, GA = 941, AA = 217; P = 0·5015). However, the age at diagnosis was significantly younger in children harbouring AA (median 2 years, range 0·83–6 years) compared with children harbouring GG (median 9·5 years, range 1·6–15 years) and GA (median 9 years, range 1–14 years) (P = 0·0094; Table I, Fig 1A). In contrast, the severity of the disease and peripheral blood cell counts were not significantly different among the *ALDH2* groups (Table I). Of the 56 children who received IST as the initial treatment, 14 of 34 in the GG group, 10 of 16 in the GA group, and 4 of 6 in the AA group underwent an HSC transplant later in the disease course. The failure-free survival rate at 10 years from IST was significantly lower in the GA/AA group (0·162, 95% confidence interval, 0·043–0·454) than in the GG group (0·467, 95% confidence interval, 0·282–0·661; P = 0·0465; Fig 1B).

ALDH2 preferentially catalyses the breakdown of acetaldehydes and other aldehydes, such as 4-hydroxynonenal and malondialdehyde, that can be genotoxic due to DNA-protein crosslinking. Recent studies have revealed that ALDH2 dysfunction may contribute to a variety of diseases and biological processes. However, to date, no study has defined the role of ALDH2 deficiency in human haematopoietic diseases in the general population.

The accumulation of DNA damage partially explains the declining function of HSCs. The type of *ALDH2* variant is associated with accelerated progression of BMF in Japanese patients with FA, and patients carrying an AA allele develop myelodysplastic syndrome with BMF at a very young age (Hira *et al*, 2013), suggesting that aldehydes are an important source of genotoxicity in the human haematopoietic system. In an FA murine model, *Aldh2*$^{-/-}$ *Fancd2*$^{-/-}$ double mutant mice spontaneously develop

doi:10.1111/bjh.13122

Table I. Patient characteristics.

	ALDH2 genotype			
	GG	GA	AA	*P*
Patients (*N*)	40	29	10	0·0094*
Age at Diagnosis, years, median (range)	9·5 (1·6–15)	9 (1–14)	2 (0·83–6)	
Gender (*N*)				
Male	23	16	8	0·8738
Female	17	13	2	
Disease Severity (*N*)				
Very severe	4	5	1	0·5453
Severe	22	12	6	
Non-severe	14	12	3	
CBC at Diagnosis				
Median WBC (x 10^9/l)	2·6	2·54	3·5	0·0587
Median ANC (x 10^9/l)	0·7	0·667	1·197	0·1879
Median Hb (g/l)	73	61	69	0·7765
Median Ret (‰)	8	16	34	0·4654
Median PLT (x 10^9/l)	11	17·5	10·5	0·3184

ALDH2, aldehyde dehydrogenase 2; CBC, complete blood cell count; WBC, white blood cell count; ANC, absolute neutrophil count; Hb, haemoglobin; Ret, reticulocyte count; PLT, platelet count.
*$P < 0·01$.

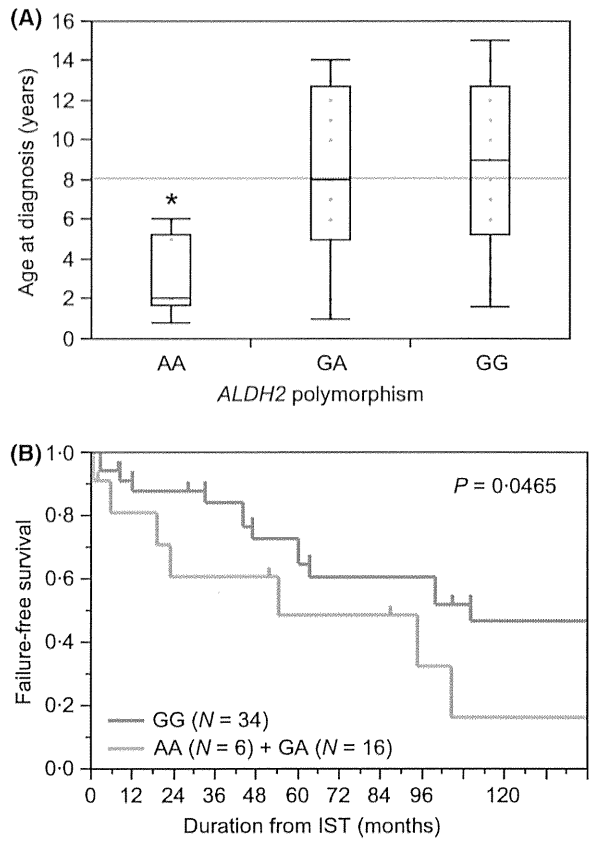

Fig 1. (A) Age at the diagnosis of idiopathic aplastic anaemia among *ALDH2* polymorphism groups. Age at diagnosis was significantly lower in the AA group harbouring a null capacity of ALDH2 (median 2 years, range 0·83–6 years) than in the GG group harbouring full capacity (median 9·5 years, range 1·6–15 years) and the GA group harbouring approximately 1/16 capacity (median 9 years, range 1–14 years). *$P = 0·0094$ with Kruskal-Wallis one-way analysis of variance. (B) Kaplan-Meier curve showing the failure-free survival (defined by survival in the absence of relapse, additional therapy, paroxysmal nocturnal haemoglobinuria, or secondary malignancy) of a cohort of 56 children who received immunosuppressive therapy (IST) for initial treatment of aplastic anaemia. The failure-free survival rate 10 years after beginning the treatment was significantly lower in the GA/AA group (0·162, 95% confidence interval, 0·043–0·454) than in the GG group (0·467, 95% confidence interval, 0·282–0·661; $P = 0·0465$, log-rank test).

aplastic anaemia due to disruption of DNA repair pathways that are required for HSC homeostasis. *Aldh2*$^{-/-}$ alone leads to a reduction in the HSC pool (Garaycoechea *et al*, 2012), indicating that endogenous aldehydes may cause an intrinsic defect in HSCs. In that study, aged *Aldh2*$^{-/-}$ *Fancd2*$^{-/-}$ double mutant mice that developed aplastic anaemia showed accumulation of damaged DNA within the HSC pool. Interestingly, *Aldh2* is dispensable for counteracting aldehydes in more mature haematopoietic precursors, suggesting that the emergence of BMF is possibly due to aldehyde-mediated genotoxicity that is restricted to HSCs.

Given that our cohort included only children (alcohol intake is not a factor), intrinsic aldehydes may play a role in accelerating BMF in children with idiopathic aplastic anaemia without other apparent genetic backgrounds that may cause intrinsic defects in HSCs. An intrinsic defect in HSCs, which is probably caused by endogenous aldehyde toxicity, may negatively affect the failure-free survival after IST in children whose aldehyde metabolism is suppressed. This intrinsic defect in HSCs is salvaged by additional treatment, most likely, HSC transplant. Our data suggest that patients with ALDH2 deficiency who are diagnosed with aplastic anaemia may need therapy in addition to conventional IST. ALDH inhibitors, such as disulfiram, may need to be avoided to retain residual ALDH2 activity in patients with low or absent ALDH2 activity. Importantly, a therapeutic approach with ALDH2 activators such as Alda-1 (Chen *et al*, 2014) may be beneficial for preventing a functional decline in HSCs.

In conclusion, endogenous aldehydes may damage HSCs, resulting in early-onset BMF in children with idiopathic aplastic anaemia. Our data suggest a novel therapeutic target for rescuing HSCs from genetic injury for the treatment of idiopathic aplastic anaemia and BMF.